IJE TRANSACTIONS C: Aspects Vol. 36 No. 06, (June 2023) 1060-1065

International Journal of Engineering

Journal Homepage: www.ije.ir

Effect of Aging Treatment on Microstructure and Mechanical Properties of Al0.7CoCrFeNi High Entropy Alloy

N. Asgarkhani, M. Seifollahi*, S. M. Abbasi

Faculty of Materials & Manufacturing Technologies, Malek Ashtar University of Technology

P A P E R I N F O

Paper history:
Received 25 January 2023
Received in revised form 15 March 2023
Accepted 16 March 2023

Keywords:
Al0.7CoCrFeNi High Entropy Alloy
Aging
Microstructure
Hardness
Hot Compression

A B S T R A C T

In this study, the effects of aging times and temperatures on the microstructure, hardness and compression strength of Al0.7CoCrFeNi high entropy alloy have been investigated. The alloy was cast in a vacuum induction melting furnace, homogenized at 1250 ˚C for 6 h; then aged at 700 to 1000˚C for 2-8 h. The as-cast structure is dendritic and includes FCC(A1) and BCC(A2, B2) phases with the hardness of 497 HV. During ageing, B2 precipitates at the grain boundaries at 700˚C and the hardness increases about 7%. The ratio of BCC to FCC phases on the basis of XRD in as-cast alloy is approximately equal which is increased by ageing at 700˚C. At 800˚C, the formation of a destructive and hard phase of σ cause to increases the hardness to 543 HV and the ratio of (A2+B2)/A1 has decreased. At 1000 ˚C, the ratio of (A2+ B2)/A1 increases, and the peak intensity of σ decreases, so that the hardness value decreases to 385 HV. The results of hot deformation test showed that the alloy at the strain rate of 10-3 s-1 and temperatures of 800, 900, 1000 and 1100˚C has a yield strength of 306, 179, 91 and 50 MPa, respectively.

***doi**: 10.5829/ije.2023.36.06c.04*

1. INTRODUCTION

The high entropy alloys are known as solid solution alloys that have 5-13 elements with the same or almost the same atomic percentage (5-35%). Solid solutions with several elements due to high entropy tend to be stable at high temperatures. It is remarkable that these alloys have low diffusion rate, which causes the formation of nanometer precipitates, and severe lattice distortion due to the difference in atomic radii [1, 2].

AlCoCrFeNi high entropy alloys have the variety of eutectic microstructures including FCC and BCC phases. The ratio of FCC to BCC phases in these alloys has a direct effect on the mechanical properties. These alloys have excellent properties such as good corrosion resistance, high hardness and elevated yield strength even at high temperatures. σ phase is the other phase in the AlCoCrFeNi alloy [1, 3]. The amount of FCC, BCC and σ phases can be controlled with chemical composition justification and heat treatment. Due to the presence of five elements, this alloy is extremely non-uniform and has dendritic structure. So, it requires high-temperature homogenization, which reduces the amount of segregation to a desirable extent and eliminates the dendritic structure [4-6].

Heat treatment process is an integral part of the industrial production components. Recent studies on high entropy alloys also show further research in this field required. Munitz et al. [7] assessed the effects of different aging temperatures on the microstructure of AlCoCrFeNi high entropy alloy. They found that aging for 3 hours at 650 ˚C, changes phases from BCC to σ and σ phase turns again to BCC at 975 ˚C. Wang et al. [8] examined the effects of aging at 600-1200 ˚C for 168 h on the microstructure of AlCoCrFeNi high entropy alloy. They found the formation of FCC phase was inhibited as a result of high rate of quenching, so the alloy maintain in solid solution manner. They also reported that after aging at temperatures of 800-1200˚C, nanometer-scale sediments and FCC phase precipitates from at the grain boundaries and cause to decrease in compressive strength and increase in ductility. Furthermore, Butler and

*Corresponding author email: m_seifollahi@mut.ac.ir (M. Seifollahi)

Please cite this article as: N. Asgarkhani, M. Seifollahi, S. M. Abbasi, Effect of Aging Treatment on Microstructure and Mechanical Properties of Al0.7CoCrFeNi High Entropy Alloy, ***International Journal of Engineering, Transactions C: Aspects***, Vol. 36, No. 06, (2023), 1060-1065

Weaver [9] reported the formation of coarse-grained microstructures consisting of FCC and BCC phases at 1050 ˚C/520 hr and stabilized FCC, BCC and σ phases at 700˚C/ 1000 h. Most of the researches conducted in the field of manufacture and characterization of alloys with different compounds or the effect of alloying elements on the microstructure and properties. In the last two years, researches have done on the effects of heat treatment [10-12] and cold work [13-15], but none of them has fully examined the mechanisms of these processes. Homogenization provides the desired microstructure for the annealing process and subsequent aging leads to the development of the service operation. Although the researchers might be assess the effects of homogenization and aging of these alloys, so there is a research gap yet. In this research, the effects of aging and its mechanism on the microstructure and hardness of Al0.7CoCrFeNi alloy were investigated.

2. MATERIALS METHOD

Al0.7CoCrFeNi alloy was melted in a vacuum induction melting (VIM) furnace under a vacuum of 3.9×10-3 Pa. The chemical composition of Al0.7CoCrFeNi alloy was measured using EDS analysis and the results are summarized in Table 1. Samples of 1×1×1 cm^3 were subjected to homogenization at 1250 ˚C for 6 h and oil quenched, then aged for 2, 4, 6 and 8 hours at temperatures of 700, 800, 900 and 1000 ˚C and water quenched. In order to study the microstructure, the samples were polished and etched in 10ml HCl+ 10ml HNO_3 + 10ml H_2O solution. The microstructure was examined by Olympus optical microscope and Vega-Tescan scanning electron microscopy equipped with EDS analysis. The hardness of the specimens was measured using a Easyway Vikers hardness testing machine under 30 kg load. Each hardness value is an average of five readings . The compression tests were performed at 800, 900 and 1100˚C using Instron 8502 machine. The samples were 8mm in diameter and 12mm in length according to ASTM E209.

3. RESULTS AND DISCUSSION

Figures 1(a) and 1(b) show the optical microstructure of cast and homogenized (1250˚C for 6 hours) Al0.7CoCrFeNi alloy, respectively. As can be seen in these figures, the casting microstructure consists of dendritic and interdendritic regions due to non-equilibrium solidification. After homogenization the microstructure becomes uniform without any dendritic morphology as a result of solid state diffusion mechanism. In Figure 1(b), the grain boundaries are perfectly clear.

TABLE 1. Chemical composition of Al0.7CoCrFeNi (at%) measured by EDS

Element	Al	Co	Cr	Fe	Ni
Nominal	17	20.75	20.75	20.75	20.75
Actual (EDS)	16.76	19.4	20.9	20.48	22.47

DSC analysis was performed on the homogenized sample up to the temperature of 1000˚C at a heating rate of 10˚C/min for 100 min under argon gas and data are shown in Figure 2. At 500˚C, a peak is observed which can be attributed to the precipitation of σ from the BCC phase. No other changes are observed due to the presence of FCC and BCC phases, which both are mixed together from the beginning and no other fuzzy transformation occurs. This is a feature of high entropy alloys that they are single-phase solid solution, and this phase is stable up to the high temperatures even close to melting temperatures [16].

Figure 3 shows the X-ray diffraction patterns of the as-cast and aged alloy at different temperatures for 4 h. The characteristic phase are summarized in Table 2. A1 and A2 are regular FCC and irregular BCC, respectively and both are rich of Co, Cr and Fe. B2 is BCC irregular phase and rich of Al and Ni.

According . Munitz et al. [7] and Wang et al. [10], it is expected that σ phase nucleated and grow at 700˚C, but it is not observed in the XRD pattern. It seems that 4 hours at 700˚C is insufficient. Of course, it is also possible that σ phase is formed at 700˚C, but its amount is less than 5% that is not detectable with XRD analysis.

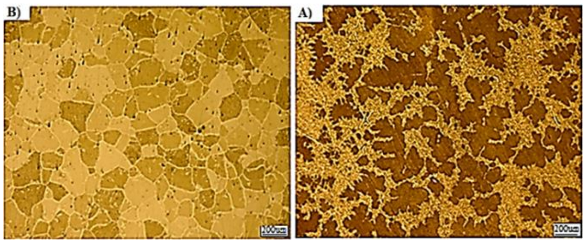

Figure 1. Optical microstructure of entropy alloy above AlCoCrFeNi (A): Casting (B): Homogenized at 1250 ˚C temperature for 6 hours and cooled in oil

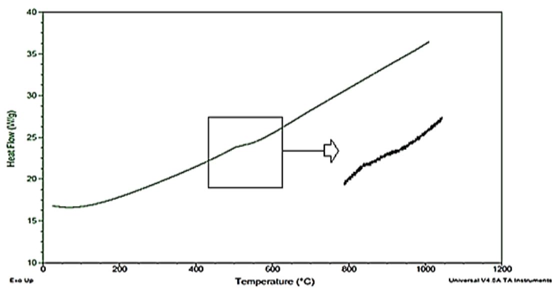

Figure 2. differential scanning calorimetry of Al0.7CoCrFeNi high entropy alloy homogenized at 1250˚C for 6 hours

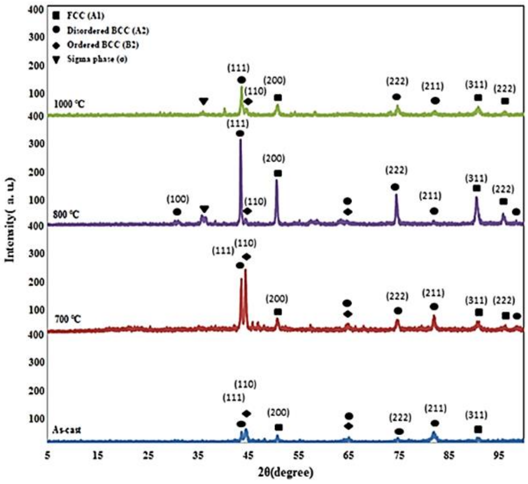

Figure 3. X-ray diffraction pattern of high entropy Al0.7CoCrFeNi after different ageing at temperatures

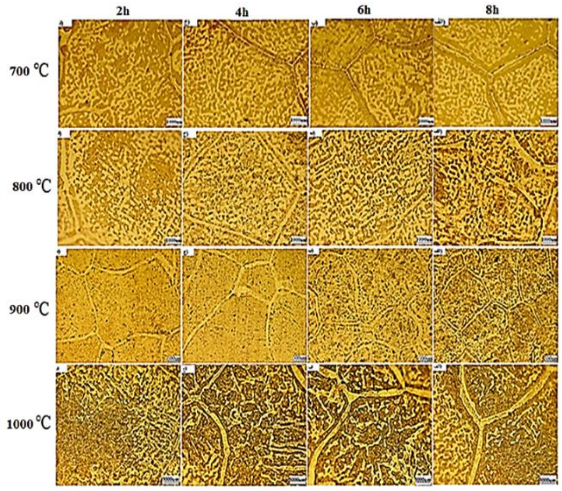

Figure 4. Optical microscopic images of AlCoCrFeNi entropy alloy after aging at temperatures of (700-1000˚C) (A: 2 h, B: 4 h, C: 6 h, D: 8) and cooled in water

TABLE 2. The characteristic of the phases measured by XRD

Heat treatment	Phases	BCC/FCC
As-cast	A1, A2, B2	1
700˚C	A1, A2, B2	2.5
800˚C	A1, A2, B2	1.7
1000˚C	A1, A2, B2, σ	2.2

As the temperature rises to 800˚C, the σ phase peak is observed in the XRD pattern. σ phase is considered harmful due to its brittle and fragile nature that forms due to the diffusion driving force increasing at 800˚C. It is possible that the formation of σ phase at 800˚C has led to the growth of FCC phase [3].

It is essential to note that dissolution of σ phase is expected at 1000˚C, and can be concluded that 4 hours is not sufficient to dissolves it. At 1000˚C the BCC/FCC ratio has been decreased due to the gradual dissolution of σ phase. Therefore, with increasing temperature up to above 1000˚C, the harmful σ phase gradually dissolves. Munitz et al. [7] reported that BCC phase converted to σ at 650˚C and to BCC again at 975˚C. σ Phase with the chemical composition of FeCr is harder than BCC and cause to hardness increase.

Figure 4 shows optical microstructure of the alloy aged at 700-1000˚C for 2-8 hours.

It is observed that after aging at 700˚C for 2h, the microstructure did not change significantly compared to the homogenized structure. The dark phase (BCC) and the white fingerprint phase (FCC) are clearly visible in the structure. At this temperature, the fraction of BCC phase is higher than FCC, which is in agreement with XRD results. It is observed that with increasing time from 2 to 8 hours, fingerprint phases tend to dissolve and join to the boundaries. Also, the thickness of the grain boundaries decreases with times. A1 (rich of Co, Cr and Fe) is a dendrites phase after solidification which dissolves and its element diffuse toward grain boundaries during homogenizing and again diffuse into B2 phase with increasing time from 2 to 8 hours.

It is noteworthy that the grain boundaries changes during ageing in comparison to homogenization and some precipitates form on the grain boundaries. According to the results of XRD analysis and also literature [7, 17], it can be said that these precipitates are B2, which is formed after aging at the grain boundaries.

At 800˚C, according to the results of XRD analysis, microstructures include FCC, BCC and σ phases. σ phases are not visible due to their small size and volume fraction. The sediments of B2 are also observed in the middle of A1. It has been reported by Wang et al. [10] that Al can stabilize the BCC phase in high entropy alloys. In particular, Al stabilizes the regular BCC (B2) and Cr stabilizes the irregular BCC (A2). The Cr greatly increases the driving force of the σ phase formation. Also, the mobility of Cr in BCC phase is much higher than in FCC. Cr by increasing the driving force plays an important role in intensifying the precipitation rate of σ. Therefore, it is expected that σ forms directly from (Fe and Cr rich FCC phase) and (Fe and Cr rich irregular BCC phase). When Cr diffuses from BCC to σ phase, at the same time, Ni atoms diffuse into the Cr depleted zones and FCC phase formed.

The microstructure of alloy aged at 900˚C is included FCC, BCC and σ phases. As can be seen in Figure 4, the microstructure has dramatically changed. It is observed that phases A1, A2, B2 are completely intertwined with each other so around the grain boundaries are sourounded by A2 and B2. It is also observed that the grain boundaries are more thicker than of 800˚C, which indicates an increase in FCC to BCC ratio due to the σ phase increasing (it will be discussed).

At 1000˚C, there are also FCC, BCC and σ phases, according to Figure 4. As can be seen in this figure, the needle like B2 precipitate are seen in the microstructures as well as around the grain boundaries. The amount of σ has been decreased, which led to a decrease in FCC, and increase in BCC phase. It is appeared that precipitates within grain boundaries are also declined slightly.

Figure 5 shows SEM images of an AlCoCrFeNi high-entropy alloy after homogenizing and aging at the temperatures of 700-1000˚C for 4 hours along with the line scan analysis of the elements.

As can be seen in Figure 5b, the depleted areas around the boundaries are disappearing in comparision to the homogenized state. In homogenized state (Figure 5(a)), the amount of Al and Ni at the grain boundaries decreases sharply, but it does not happen in aged sample due to the deposition of B2 inside A1 after aging.

Figure 5(c) shows the extensive amount of needle-liked BCC phase, which are scattered throughout the microstructure. The BCC phase is appeared to accumulate and move toward boundaries as temperature rises. It is also observed that the fingerprint phases also tend to approach the boundaries. Until 700˚C, the boundaries are free from dark BCC phases. As the temperature increases, due to BCC to σ phase transformation, the morphology of BCC phases changes from the coarse fingerprint to needle-liked which indicates a decrease in BCC to FCC ratio. The results of

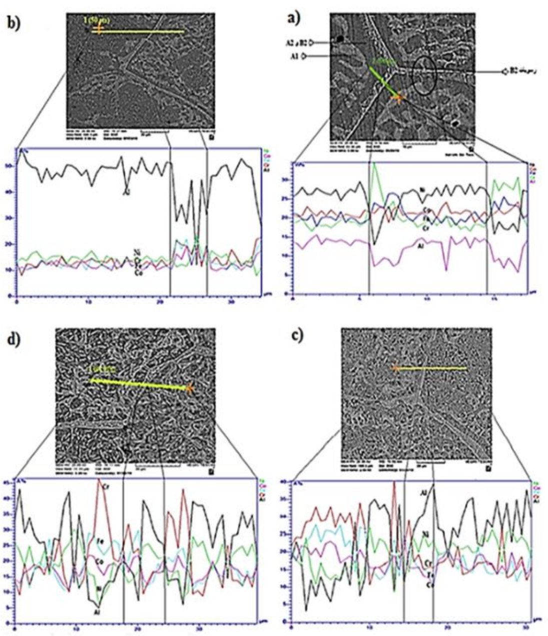

Figure 5. Electron microscopic images of an AlCoCrFeNi entropy alloy overgrown after aging at temperatures of 700 to 1000˚C (a-d, respectively) for 4 hours and cooled in water with a linear analysis of the distribution of their elements

In Figure 5(c), Al, Co, Cr, Fe and Ni elements are scattered throughout the microstructure. At the grain boundaries, Al and Ni have increased and Co, Cr and Fe have slightly decreased. Therefore, it can be concluded that with increasing aging temperature to 900˚C, B2 has penetrated more into the boundaries, which is also observed in Figure 5(c).

As can be seen in Figure 5(d), at 1000˚C, B2 phase is scattered through the boundaries, and in fingerprint phases. So, it can be said that phase B2 has penetrated into phase A1. B2 appear to get more elongated at 1000˚C. The results of linear element analysis also show that all the elements are mixed together and it is difficult to separate them from each other.

Figure 6 shows the variation of hardness during ageing from 700 to 1000˚C. after ageing, hardness increase until 800˚C and again started to decrease until 1000˚C.
linear scan analysis indicate that needle like phases are rich of Al and Ni. Needle like BCC and B2 are enrich of Al and Ni, respectively. The different behavior between Al and Ni is related to the diffusion coefficient of the elements. Al has superior diffusion coefficient compared to Ni [18], so, Al has diffused to the grain boundaries more.

The fast increase in hardness is due to an increase in BCC to FCC ratio and possibly the precipitation of σ. at 800˚C, the hardness increased to 543 HV, which is due to the formation of needle like B2 phase and σ. At 900 and 1000˚C, the hardness decreased to 454 and 385 HV, respectively, which is due to the gradual dissolution of phase σ. The σ phase is a hard and brittle phase with FeCr composition. This phase precipitates with slow diffusion mechanism at 700˚C cause to increases hardness. This phase tends to dissolve as the temperature rises and dissolves completely at 1250˚C [18-21].

The flow curve of hot compression test of the alloy is shown in Figure 7. The results showed that the alloy at 800, 900, 1000 and 1100˚C has a yield strength of 306, 179, 91 and 50 MPa, respectively. At the beginning of the deformation, with increasing strain, the stress increases linearly until it reaches the yield point. Then, as the strain increases, the density of dislocations increases and hardening occurs. As the deformation continues, the heat energy during the hot work leads to a smooth dynamic recovery mechanism. With increasing

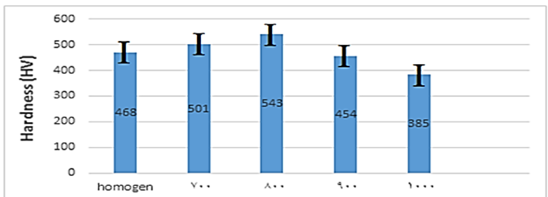

Figure 6. Chart of hardness changes of homogenized and aged samples at temperatures of 700, 800, 900 and 1000˚C for 2, 4, 6, 8 hours and cooled in water

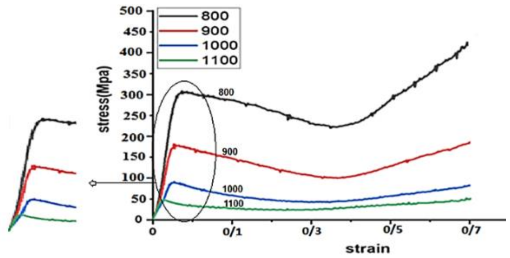

Figure 7. True compressive stress-strain diagram of alloy under different heat treatment conditions

temperature, the hardness gradually decreases and reaches to a stable state. In the early stages of deformation, the occurrence of recovery is not able to fully cope with the hardness and therefore the hardness increases. As the strain increases, the slope of the stress-strain curve increases and the stiffness decreases significantly. This process continues to reach the maximum point. In this case, the density of the dislocations is increased so the recovery overcomes the stiffness and the flow stress decreases to reach the steady state. In this case, the balance between the rate of dislocations formation and elimination occured and the tension remains constant.

4. CONCLUSIONS

1. The results of XRD phase analysis show that the high entropy alloy of AlCoCrFeNi has 3 phases FCC (A1), BCC (A2, B2) and σ. The ratio of BCC and FCC phases in the as cast structure is approximately equal. After aging at 700˚C, 800˚C and 1000˚C the ratio of BCC to FCC phase is about 2.5, 1.7 and 2.2, respectively
2. The peak at 500˚C in the DSC thermal analysis results is attributed to the precipitation of phase σ from the BCC phase, which is re-dissolved at a temperature of about 1000˚C.
3. After aging at 700˚C, fingerprint phases tend to join the boundaries, and deposits of the B2 phase form within the boundaries.
4. At 800˚C, fingerprint phases are mixed with borders and forms the needle-shaped sediments in phase B2 and also σ.
5. As a result of microstructure changes during aging, the hardness of the alloy changes from 467Hv in the as cast structure to 501, 543, 454 and 385Hv at aging temperature of 700, 800, 900 and 1000˚C respectively.
6. The results of hot compression test showed that the alloy at 800, 900, 1000 and 1100˚C has a yield strength of 306, 179, 91 and 50 MPa, respectively.

5. REFERENCES

1. Niu, P., Li, R., Yuan, T., Zhu, S., Chen, C., Wang, M. and Huang, L., "Microstructures and properties of an equimolar alcocrfeni high entropy alloy printed by selective laser melting", ***Intermetallics***, Vol. 104, (2019), 24-32. doi: 10.1016/j.intermet.2018.10.018.
2. Vyas, A., Menghani, J. and Natu, H., "Metallurgical and mechanical properties of laser cladded alfecucrconi-wc10 high entropy alloy coating", ***International Journal of Engineering, Transactions A: Basics***, Vol. 33, No. 7, (2020), 1397-1402. doi: 10.5829/IJE.2020.33.07A.27.
3. Murty, B.S., Yeh, J.-W., Ranganathan, S. and Bhattacharjee, P., "High-entropy alloys, Elsevier, (2019).
4. Shi, Y., Collins, L., Feng, R., Zhang, C., Balke, N., Liaw, P.K. and Yang, B., "Homogenization of alxcocrfeni high-entropy alloys with improved corrosion resistance", ***Corrosion Science***, Vol. 133, (2018), 120-131. doi: 10.1016/j.corsci.2018.01.030.
5. Wei, L., Liu, X., Gao, Y., Peng, X., Hu, N. and Chen, M., "Phase, microstructure and mechanical properties evaluation of alcocrfeni high-entropy alloy during mechanical ball milling", ***Intermetallics***, Vol. 138, (2021), 107310. doi: 10.1016/j.intermet.2021.107310.
6. Zhao, C., Li, J., Liu, Y., Ma, X., Jin, Y., Wang, W.Y., Kou, H. and Wang, J., "Optimizing mechanical and magnetic properties of alcocrfeni high-entropy alloy via fcc to bcc phase transformation", ***Journal of Materials Science & Technology***, Vol. 86, (2021), 117-126. doi: 10.1016/j.jmst.2020.12.080.
7. Munitz, A., Salhov, S., Hayun, S. and Frage, N., "Heat treatment impacts the micro-structure and mechanical properties of alcocrfeni high entropy alloy", ***Journal of Alloys and Compounds***, Vol. 683, (2016), 221-230. doi: 10.1016/j.jallcom.2016.05.034.
8. Wang, R., Zhang, K., Davies, C. and Wu, X., "Evolution of microstructure, mechanical and corrosion properties of alcocrfeni high-entropy alloy prepared by direct laser fabrication", ***Journal of Alloys and Compounds***, Vol. 694, (2017), 971-981. doi: 10.1016/j.jallcom.2016.10.138.
9. Butler, T.M. and Weaver, M.L., "Investigation of the phase stabilities in alnicocrfe high entropy alloys", ***Journal of Alloys and Compounds***, Vol. 691, (2017), 119-129. doi: 10.1016/j.jallcom.2016.08.121.
10. Wang, W.-R., Wang, W.-L. and Yeh, J.-W., "Phases, microstructure and mechanical properties of alxcocrfeni high-entropy alloys at elevated temperatures", ***Journal of Alloys and Compounds***, Vol. 589, (2014), 143-152. doi: 10.1016/j.jallcom.2013.11.084.
11. Toocharoen, S., Kaewkuekool, S. and Peasura, P., "The rejuvenation heat treatment of nickel base superalloy grade gtd111 after long-term service via the taguchi method for optimization", ***International Journal of Engineering, Transactions A: Basics***, Vol. 34, No. 4, (2021), 956-965. doi: 10.5829/IJE.2021.34.04A.22.
12. Azadi, M., Iziy, M., Marbout, A. and Rizi, M., "Investigation of the heat treatment effect on microstructures and phases of inconel 713c superalloy", ***International Journal of Engineering, Transactions A: Basics***, Vol. 30, No. 10, (2017), 1538-1544. doi: 10.5829/ije.2017.30.10a.15.
13. Gwalani, B., Soni, V., Lee, M., Mantri, S., Ren, Y. and Banerjee, R., "Optimizing the coupled effects of hall-petch and precipitation strengthening in a al0. 3cocrfeni high entropy alloy", ***Materials & Design***, Vol. 121, (2017), 254-260. doi: 10.1016/j.matdes.2017.02.072.
14. Kuwabara, K., Shiratori, H., Fujieda, T., Yamanaka, K., Koizumi, Y. and Chiba, A., "Mechanical and corrosion properties of alcocrfeni high-entropy alloy fabricated with selective electron beam melting", ***Additive Manufacturing***, Vol. 23, (2018), 264-271. doi: 10.1016/j.addma.2018.06.006.
15. Tang, Z., Senkov, O.N., Parish, C.M., Zhang, C., Zhang, F., Santodonato, L.J., Wang, G., Zhao, G., Yang, F. and Liaw, P.K.,

"Tensile ductility of an alcocrfeni multi-phase high-entropy alloy through hot isostatic pressing (HIP) and homogenization", ***Materials Science and Engineering: A***, Vol. 647, (2015), 229-240. doi: 10.1016/j.msea.2015.08.078.

16. Zhao, C., Li, J., Liu, Y., Wang, W.Y., Kou, H., Beaugnon, E. and Wang, J., "Tailoring mechanical and magnetic properties of alcocrfeni high-entropy alloy via phase transformation", ***Journal of Materials Science & Technology***, Vol. 73, (2021), 83-90. doi: 10.1016/j.jmst.2020.08.063.
17. Strumza, E. and Hayun, S., "Comprehensive study of phase transitions in equiatomic alcocrfeni high-entropy alloy", ***Journal of Alloys and Compounds***, Vol. 856, (2021), 158220. doi: 10.1016/j.jallcom.2020.158220.
18. Vaidya, M., Trubel, S., Murty, B., Wilde, G. and Divinski, S.V., "Ni tracer diffusion in cocrfeni and cocrfemnni high entropy alloys", ***Journal of Alloys and Compounds***, Vol. 688, (2016), 994-1001. doi: 10.1016/j.jallcom.2016.07.239.
19. Shivam, V., Basu, J., Pandey, V.K., Shadangi, Y. and Mukhopadhyay, N., "Alloying behaviour, thermal stability and phase evolution in quinary alcocrfeni high entropy alloy", ***Advanced Powder Technology***, Vol. 29, No. 9, (2018), 2221-2230. doi: 10.1016/j.apt.2018.06.006.
20. Joseph, J., Hodgson, P., Jarvis, T., Wu, X., Stanford, N. and Fabijanic, D.M., "Effect of hot isostatic pressing on the microstructure and mechanical properties of additive manufactured alxcocrfeni high entropy alloys", ***Materials Science and Engineering: A***, Vol. 733, (2018), 59-70. doi: 10.1016/j.msea.2018.07.036.
21. Uporov, S., Bykov, V., Pryanichnikov, S., Shubin, A. and Uporova, N., "Effect of synthesis route on structure and properties of alcocrfeni high-entropy alloy", ***Intermetallics***, Vol. 83, (2017), 1-8. doi: 10.1016/j.intermet.2016.12.003.

Persian Abstract

چکیده

در این پژوهش، اثر دما وزمان پیرسازی بر ریزساختار،سختی و استحکام فشاری آلیاژ آنتروپی بالای Al0.7CoCrFeNi مورد بررسی قرار گرفته است. آلیاپ به روش ذوب القایی تحت خلأ تولید و در دمای $^{\circ}C$ ۱۲۵۰ به مدت ۲ ساعت همگن سازی شده است. سپس در دمای $^{\circ}C$ ۱۰۰۰–۷۰۰ تحت عملیات پیرسازی قرار گرفته است.ساختار ریختگی به صورت دندریتی و شامل فازهای $FCC(A_1)$ و$BCC(A_2,B_2)$ با سختی ٤۹۷ ویکرز است. پس از پیرسازی در دمای ۷۰۰$^{\circ}C$، فاز B_2 رسوب کرده و نسبت فازهای BCC به FCC که در حالت ریختگی تقریبا برابر یک است، زیاد می‌شود. در ۸۰۰$^{\circ}C$، فاز مخرب و سخت σ تشکیل شده وسختی به ٥٤۳ ویکرز رسیده و نسبت (A2+B2)/A1 کاهش می‌یابد. در ۱۰۰۰$^{\circ}C$، این نسبت، میزان σ و سختی تا ۳۸۵ ویکرز کاهش می‌یابد. نتایج آزمایش فشار گرم نشان داد که آلیاژ دارای استحکام ۳۰٦ ، ۱۷۹، ۹۱ و ٥۰MPa به ترتیب در دماهای ۸۰۰، ۹۰۰، ۱۰۰۰ و$^{\circ}C$ ۱۱۰۰ است.